THE ANNALS OF "DUNAREA DE JOS" UNIVERSITY OF GALATI
FASCICLE V, TECHNOLOGIES IN MACHINE BUILDING,
ISSN 1221- 4566

INTERFERENCE BETWEEN PROFILES – GRAPHICAL ALGORITHM IN CATIA BY THE METHOD OF GENERATING TRAJECTORIES FAMILY

Nicuşor BAROIU, Virgil Gabriel TEODOR,
Florin SUSAC, Nicolae OANCEA

Department of Manufacturing Engineering, Dunarea de Jos University of Galati
nicusor.baroiu@ugal.ro

ABSTRACT

A shortcoming of generation using rolling method is given by the interference of profiles due to the generation of trajectories of the discontinuities on the composed profiles, as happens with the majority of profiles used in technical applications.

An analysis of an interference process in case of a gear worm is proposed in this paper. The problem is approached as a gear between the toothed wheel and the rack (the worm's axial section), using the complementary theorem of the generation of trajectories. An analytical support and a graphical algorithm developed in CATIA design environment are presented. A numerical example calculated using the graphical methodology is also presented.

KEYWORDS: interference, graphical method, CATIA, generating trajectories family

1. INTRODUCTION

The interference of surfaces (profiles) generated by surface enwrapping machining techniques is one of the limits of this generating process. The profiles' interference is due to the presence on the technical profiles, which, frequently, are composed profiles, of singular points — points where two distinct normals can be defined.

Due to this cause, the enwrapping condition definition in these points is ambiguous; consequently, considering the inherent discontinuities onto the tool's profile, the relative trajectory generation regarding the tool or the blank creates forms which lead to interference of profiles.

In order to avoid these generating trajectories it is mandatory to make discontinuities onto profiles. This is difficult to realize from a technical point of view [1], [9].

The dimensions of the transition curves — generating trajectories of the singular points — can be limited changing the form of the centrodes associated with profiles at generation by rolling, the constructive modification of the surface to be generated for helical surfaces, generation of one surface with multiple tools, in successive passages. All these methods are difficult to realize in practical execution of surface generation.

The issue of surfaces (profiles) interference generated by enwrapping is frequently presented in specialized literature in order to elaborate solutions for identification of the interference zones onto profiles and ways to diminish the influence of the interference process on the functionality of generated surfaces. Regarding the analytical methods for the study of profiles interference, Zhang [3] proposes a solution for this problem using the "finite element method (FEM) for the three-dimensional stress analysis at interference titled connections". This leads to increased accuracy of results in comparison with classical methods.

Also, Pimsarn [4] proposes a new estimation method for pseudo-interference stiffness. The proposed method is faster and more accurate than the finite element method applied for solids in contact.

At the same time, authors like He Guiping and all [5] present graphical solutions for determining the interference between profiles at machining of non-circular toothed wheels.

Similar problems are presented by Berbinschi and all [6], with solutions developed in CATIA.

An issue related to assembling interference for a worm gear is approached in this paper, and a graphical solution in CATIA is presented.

2. ENWRAPPING PROFILES

An analysis of a worm gear is proposed. The approach is based on the axial section gearing (rack-gear) with the crossing section, in the same plane, of the cylindrical wheel (figures 1a and 1b).

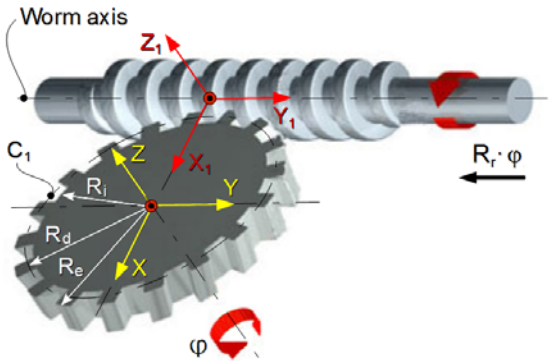

a.

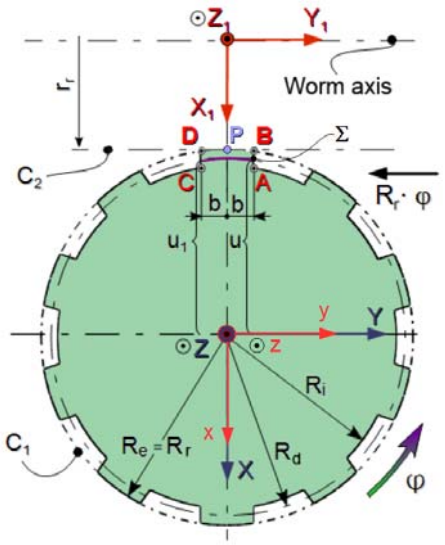

b.

Fig. 1. *The worm-cylindrical wheel gear:* ***a.*** *gearing kinematics;* ***b.*** *wheel's profile, rolling centrodes and reference systems*

The reference systems are defined:

XYZ is the relative reference system joined with the C_1 centrode of the cylindrical wheel (*Z* is the rotation axis);

$X_1Y_1Z_1$ — relative reference system joined with the C_2 centrode of the reference rack-gear (axial section of the worm); Y_1 — worm's axis. The *XY* and X_1Y_1 planes are identical.

xyz — global reference system. Initially the axes of the XYZ relative reference system overlap with the axes of the global reference system.

In Figure 1b, the relative reference systems are represented in the initial position.

In the *XY* reference system are defined the Σ surfaces for the two flanks: $\overline{AB}$ (right flank) and, respectively $\overline{CD}$ (left flank).

$$\Sigma_{AB}\begin{vmatrix} X=-u; \\ Y=b; \\ Z=h. \end{vmatrix} \quad (1)$$

$$\Sigma_{CD}\begin{vmatrix} X=-u_1; \\ Y=-b; \\ Z=h. \end{vmatrix} \quad (2)$$

The *h* parameter in the generating plane has value 0 ($h=0$).

The variation limits for the *u* parameter are:

$$u_{\min}=\sqrt{R_i^2-b^2}\,;\quad u_{\max}=\sqrt{R_e^2-b^2} \quad (3)$$

and similarly for u_1.

It is known that, for this profile type, the minimum value of the rolling radius is u_{max}.

According to the generating trajectory method [7], the versor of the normal to the $\sum$ surface is calculated:

$$\vec{N}_{\Sigma_{AB}}=\begin{vmatrix} \vec{i} & \vec{j} & \vec{k} \\ -1 & 0 & 0 \\ 0 & 0 & 1 \end{vmatrix}=\vec{j} \quad (4)$$

and, similarly,

$$\vec{N}_{\Sigma_{CD}}=\vec{j}\,. \quad (5)$$

Now, the equations of normals to the flanks Σ_{AB} and Σ_{CD} can be written in the current point:

$$N_{\Sigma_{AB}}\begin{vmatrix} X=-u; \\ Y=b+\lambda; \\ Z=h, \end{vmatrix} \quad (6)$$

and, similarly,

$$N_{\Sigma_{CD}}\begin{vmatrix} X=-u_1; \\ Y=-b+\lambda; \\ Z=h, \end{vmatrix} \quad (7)$$

where λ is a variable scalar parameter.

The relative motion between the $X_1Y_1Z_1$ and *XYZ* reference systems is given by transformation:

$$X_1=\omega_3^T(\varphi)\cdot X-a\,, \quad (8)$$

where

$$\omega_3^T(\varphi)=\begin{Vmatrix} \cos\varphi & -\sin\varphi & 0 \\ \sin\varphi & \cos\varphi & 0 \\ 0 & 0 & 1 \end{Vmatrix};\quad a=\begin{Vmatrix} -(R_r+r_r) \\ -R_r\cdot\varphi \\ 0 \end{Vmatrix}. \quad (9)$$

In this way, from (8) with definitions (9), the family of normals to the $\overline{AB}$ and $\overline{CD}$ flanks is defined in the forms:

$\overline{AB}$ flank:

$$\begin{Vmatrix} X_1 \\ Y_1 \\ Z_1 \end{Vmatrix}=\begin{Vmatrix} \cos\varphi & -\sin\varphi & 0 \\ \sin\varphi & \cos\varphi & 0 \\ 0 & 0 & 1 \end{Vmatrix}\cdot\begin{Vmatrix} -u \\ b+\lambda \\ H \end{Vmatrix}-\begin{Vmatrix} -(R_r+r_r) \\ -R_r\cdot\varphi \\ 0 \end{Vmatrix}, \quad (10)$$

$$\left(N_{\Sigma_{AB}}\right)_{\varphi}\begin{vmatrix} X_1=-u\cdot\cos\varphi-(b+\lambda)\cdot\sin\varphi+(R_r+r_r); \\ Y_1=-u\cdot\sin\varphi+(b+\lambda)\cdot\cos\varphi+R_r\cdot\varphi; \\ Z_1=h. \end{vmatrix} \quad (11)$$

$\overline{CD}$ flank:

$$\begin{Vmatrix} X_1 \\ Y_1 \\ Z_1 \end{Vmatrix} = \begin{Vmatrix} \cos\varphi & -\sin\varphi & 0 \\ \sin\varphi & \cos\varphi & 0 \\ 0 & 0 & 1 \end{Vmatrix} \cdot \begin{Vmatrix} -u_1 \\ -b+\lambda \\ H \end{Vmatrix} - \begin{Vmatrix} -(R_r + r_r) \\ -R_r \cdot \varphi \\ 0 \end{Vmatrix}, \quad (12)$$

$$\left(N_{\Sigma_{CD}}\right)_{\varphi} \begin{cases} X_1 = -u_1 \cdot \cos\varphi - (-b+\lambda)\cdot\sin\varphi + (R_r + r_r); \\ Y_1 = -u_1 \cdot \sin\varphi + (-b+\lambda)\cdot\cos\varphi + R_r \cdot \varphi; \\ Z_1 = h. \end{cases} \quad (13)$$

For $\lambda=0$, equations (11) and (13) represent the generating trajectories of points belonging to the toothed wheel profiles.

The enwrapping of generating trajectories represents the rack-gear profile (axial section of the worm from construction of the analysed gear).

In order to determine the enwrapping condition, it is imposed that the normals family (11) and (13) pass through the incident line to the gearing pole of the in-plane gearwheel-rack gear (axial section of the worm), which is perpendicular to the XY plane and has the following coordinates:

$$P \begin{cases} X_1 = r_r; \\ Y_1 = R_r \cdot \varphi; \\ Z_1 = 0. \end{cases} \quad (14)$$

In this way, from (11) and (14) result the conditions:

$$\begin{aligned} -u\cdot\cos\varphi - (b+\lambda)\cdot\sin\varphi + (R_r + r_r) &= r_r; \\ -u\cdot\sin\varphi + (b+\lambda)\cdot\cos\varphi + R_r\cdot\varphi &= R_r\cdot\varphi. \end{aligned} \quad (15)$$

Removing the λ parameter between the two equations

$$\frac{-u\cdot\cos\varphi + R_r - b\cdot\sin\varphi}{\sin\varphi} = \frac{-u\cdot\sin\varphi + b\cdot\cos\varphi}{-\cos\varphi}, \quad (16)$$

from the enwrapping condition results:

$$u = R_r \cdot \cos\varphi. \quad (17)$$

For $\lambda=0$, the equations assembly (11) and (17) represents the enwrapping of generating trajectories, namely the conjugated rack-gear's profile (worm's axial section, $h=0$).

The problem is similar for CD flank.

The profile of the worm's axial section results from (11) and (17):

$$S_{AB} \begin{cases} X_1 = -R_r \cdot \cos^2\varphi - b\cdot\sin\varphi + (R_r + r_r); \\ Y_1 = -R_r \cdot \sin\varphi\cdot\cos\varphi + b\cdot\cos\varphi + R_r\cdot\varphi; \\ Z_1 = 0. \end{cases} \quad (18)$$

Similarly, for left flank CD:

$$S_{CD} \begin{cases} X_1 = -R_r \cdot \cos^2\varphi + b\cdot\sin\varphi + (R_r + r_r); \\ Y_1 = -R_r \cdot \sin\varphi\cdot\cos\varphi - b\cdot\cos\varphi + R_r\cdot\varphi; \\ Z_1 = 0, \end{cases} \quad (19)$$

and, as well,

$$S_{BD} \begin{cases} X_1 = r_r + R_r - R_e; \\ Y_1 = R_r \cdot \varphi; \\ Z_1 = 0. \end{cases} \quad (20)$$

The worm's analytical model

The worm's axial section in helical motion around Y_1 axis, with p helical parameter, generates the helical cylindrical worm, right hand worm.

The helical movement of the worm's axial section is described by a transformation in the form:

$$X_1 = \omega_2^T(v)\cdot X_{1_{AB}} + p\cdot v\cdot\vec{j}, \quad (21)$$

with $X_{1_{AB}}$ from (18) and, similarly, for $\overline{BD}$ and $\overline{CD}$ (see (19) and (20)).

Finally, after developments, the analytical forms result:

$$S_{DB} \begin{cases} X_1 = (R_r + r_r - R_e)\cdot\cos v; \\ Y_1 = R_r\cdot\varphi + p\cdot v; \\ Z_1 = (R_r + r_r - R_e)\cdot\sin v. \end{cases} \quad (22)$$

$$S_{AB} \begin{cases} X_1 = \left(R_r\cdot\sin^2\varphi - b\cdot\sin\varphi + r_r\right)\cdot\cos v; \\ Y_1 = -R_r\cdot\sin\varphi\cdot\cos\varphi + b\cdot\cos\varphi + R_r\cdot\varphi + p\cdot v; \\ Z_1 = -\left(R_r\cdot\sin^2\varphi - b\cdot\sin\varphi + r_r\right)\cdot\sin v. \end{cases} \quad (23)$$

$$S_{CD} \begin{cases} X_1 = \left(R_r\cdot\sin^2\varphi + b\cdot\sin\varphi + r_r\right)\cdot\cos v; \\ Y_1 = -R_r\cdot\sin\varphi\cdot\cos\varphi - b\cdot\cos\varphi + R_r\cdot\varphi + p\cdot v; \\ Z_1 = \left(-R_r\cdot\sin^2\varphi - b\cdot\sin\varphi + r_r\right)\cdot\sin v. \end{cases} \quad (24)$$

3. THE INTERFERENCE STUDY

The gear between the worm and the cylindrical wheel, with straight lined frontal profile, has a certain thickness; let this be 2H (see figure 2).

In this way, due to the worm's helical flanks, interference can occur. These interferences can affect the gear's proper functioning.

In principle, the equations which describe the "gearing" process between the generating trajectories (18) and (19) from the reference plane but "raised" with elevation h (see figure 2), and the surfaces of the helical flanks S_{AB} and S_{CD} (see (22), (23) and (24)).

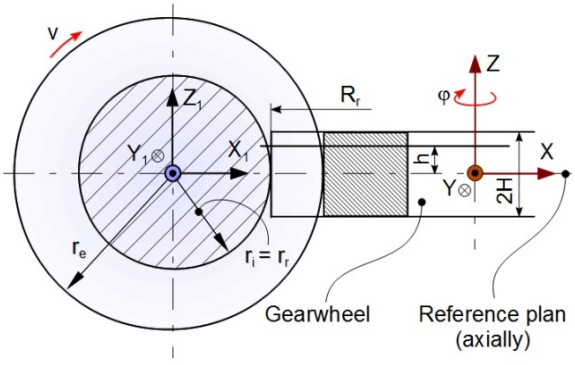

Fig. 2. *Worm gear with defined thickness*

In this way, the determining of interference zones assumes solving the equations systems of the two surfaces:

- the helical surface for the two flanks (see equations (23) and (24));

- the cylindrical surface representing the geometric locus of the family of generating trajectories (see equations (18) and (19)) for $\lambda=0$.

- the equations of all these surfaces must be reported to a same reference system; let this be $X_1Y_1Z_1$.

The conditions for the assembling interference study assume the determination of some constant values, firstly, the worm's helical parameter.

We assume that the gearwheel has k teeth (k integer) and, therewith, the gap between two teeth of the circle with radius R_r is equal with the tooth thickness.

In this way, the circular pitch, p_c, is:

$$p_c = \frac{2\pi \cdot R_r}{k} . \qquad (25)$$

Obviously, from the two centrodes rolling condition, the circular pitch (25) is equal with the worm's axial pitch, so, the helical parameter results:

$$p = \frac{2\pi \cdot R_r}{k} \cdot \frac{1}{2\pi} = \frac{R_r}{k} . \qquad (26)$$

The assembling interference is given by the impossibility to approach the toothed wheel to the conjugated worm.

For the *CD* flank the interference determining conditions are (28), see (24) for the worm's flank and (2) for the toothed wheel's flank.

The equations system has as unknown values: u, h. Among these, u is arbitrary value.

So, the system is determined and the value of the h parameter, for which the interference emerges, can be established.

In principle, the interference is the intersection curve between the helical flanks of the worm and the wheel's flanks.

The interference condition for $\overline{AB}$ straight line segment:

$$\begin{cases} \left(R_r \cdot \sin^2 \varphi - b \cdot \sin\varphi + r_r\right) \cdot \cos v = -u; \\ -R_r \cdot \sin\varphi \cdot \cos\varphi + b \cdot \cos\varphi + R_r \cdot \varphi + p \cdot v = b; \\ \left(R_r \cdot \sin^2 \varphi - b \cdot \sin\varphi + r_r\right) \cdot \sin v = h. \end{cases} \qquad (27)$$

The interference condition for $\overline{CD}$ straight line segment:

$$\begin{cases} \left(R_r \cdot \sin^2 \varphi - b \cdot \sin\varphi + r_r\right) \cdot \cos v = \\ = -u \cdot \cos\delta - b \cdot \sin\delta; \\ -R_r \cdot \sin\varphi \cdot \cos\varphi - b \cdot \cos\varphi + R_r \cdot \varphi + p \cdot v = \\ = u \cdot \sin\delta + b \cdot \cos\delta; \\ \left(R_r \cdot \sin^2 \varphi - b \cdot \sin\varphi + r_r\right) \cdot \sin v = h. \end{cases} \qquad (28)$$

The basic algorithm proves the difficulty to solve the interference problem in analytical way. This is due to the fact that the equations which describe the problem are transcendental equations.

An easier way is the graphical one. In following is presented an algorithm and applications developed in a graphical design environment.

4. GRAPHICAL METHOD

A graphical method for determining the assembling interference was developed in CATIA.

The imagined algorithm assumes that, starting from the known profile of the wheel, the axial worm's profile is calculated. This stage is made using the kinematical method for rack-gear tool's profiling [6].

Consequently, the worm's axial profile is moved along the directrix helix using the *SWEEP* command.

In this way, one of the helical surface's flanks is generated.

In the same file, where the helical surface is represented, the cylindrical surface of the wheel's flank is generated.

The intersection between the worm's flank and the wheel's flank will represent the interference curve. This curve is obtained with the *INTERSECTION* command.

The coordinates of the points on the interference curve can be obtained defining an auxiliary plane at distance h from the *XOY* plane. The intersection between this plane and the interference curve can be obtained using again the *INTERSECTION* command and represents the searched point onto the interference curve.

The coordinates of this point can be determined using the *MEASURE ITEM* command.

The presented algorithm was applied for a worm with characteristic dimensions (see figure 1.b): R_e=62.5 mm; R_i=56 mm; b=9 mm; H=5 mm; r_r=60 mm; z=1 start of worm; k=10 teeth of wheel and R_r=62.5 mm.

The form and coordinates of the interference curve are given in Figures 3.a, 3.b and Table 1.

Table 1. *Coordinates of points from the interference curve*

Crt. no.	X_1 [mm]	Y_1 [mm]	Z_1 [mm]
1	62.411	9	5.0
2	62.274	9	4.5
3	62.128	9	4.0
4	62.971	9	3.5
5	61.802	9	3.0
6	61.620	9	2.5
7	61.420	9	2.0
8	61.199	9	1.5
9	60.952	9	1.0
10	60.668	9	0.5

In order to reduce the length of the interference curve it is possible to increase the worm's diameter.

The results for the interference curve in case of r_r=120 mm are presented in Table 2 and Figure 4.

Table 2. *Coordinates of points from the interference curve*

Crt. no.	X_1 [mm]	Y_1 [mm]	Z_1 [mm]
1	121.582	9	5.0
2	121.492	9	4.5
3	121.397	9	4.0
4	121.296	9	3.5
5	121.188	9	3.0
6	121.072	9	2.5
7	120.948	9	2.0
8	120.814	9	1.5
9	120.667	9	1.0
10	-	-	-

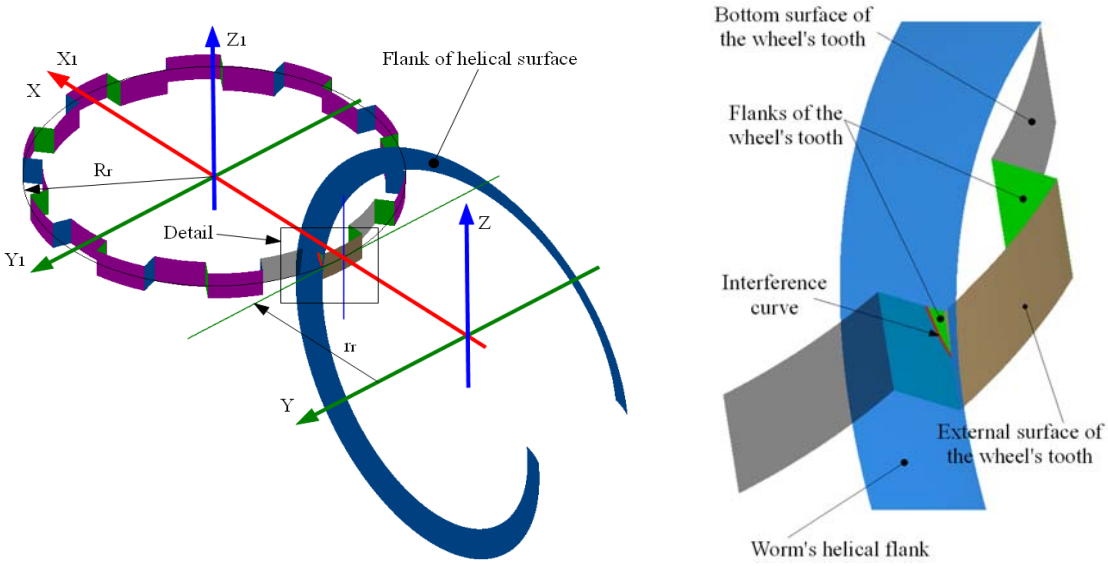

Fig. 3. *3D model of the flanks' surfaces:*
a) *assembling interference;* b) *detail of the interference zone*

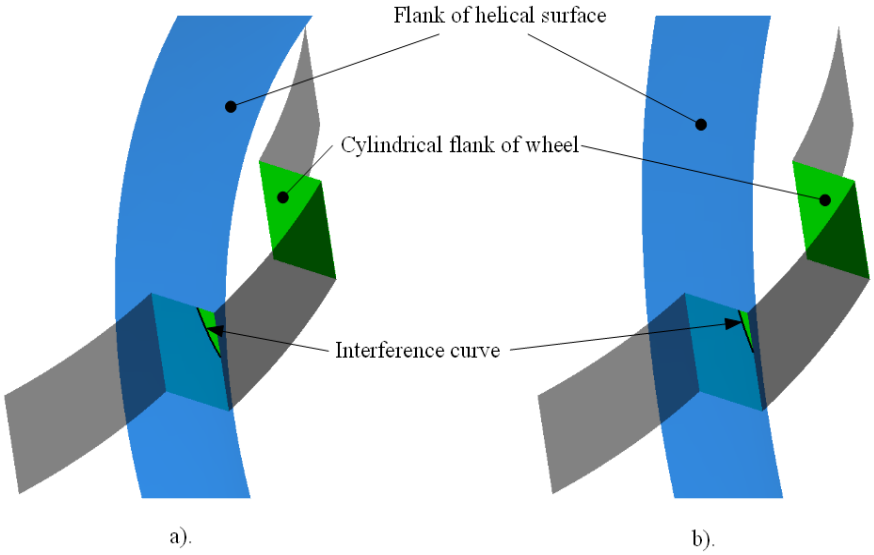

Fig. 4. *Length of the assembling interference curve: a) r_r=60 mm; b) r_r=120 mm*

5. CONCLUSIONS

An analysis of an interference process, in case of a gear worm is approached as a gear between the toothed wheel and the rack (the worm's axial section), using the complementary theorem of the generating trajectories.

An analytical support and, in the same time, a graphical algorithm developed in CATIA design environment are presented.

A numerical example calculated using the graphical methodology is also presented.

The graphical method allows changing the gearing parameters, as helical pitch, worm radius, rolling radius, etc.

We can observe that increasing the rolling radius of the worm (r_r) the length of the interference curve decreases.

As it is visible from Tables 1 and 2, below a certain value of the wheel thickness (the h parameter) the interference does not appear. This value increases with the value of r_r. For example, if r_r=60 mm, the interference emerges for values of h above 0.5 mm (table 1) while if r_r=120 mm the interference emerges for values of h above 1 mm (table 2).

Moreover, if the wheel's flank is inclined, the interference can be reduced, even avoided.

ACKNOWLEDGEMENT

This work was supported by a grant of the Romanian National Authority for Scientific Research and Innovation, CNCS – UEFISCDI, project number PN-II-RU-TE-2014-4-0031.

REFERENCES

[1] Litvin, F.L., *Theory of Gearing, Reference Publication 1212 NASA*, Scientific and Technical Information Division, Washington D.C., 1984.

[2] Oancea, N., *Surfaces generation by enwrapping*, Vol. I, II, „Dunărea de Jos" University Foundation Publishing House, ISBN 973-627-106-4, Galați, 2004.

[3] Zhang Y., McClain B. and Fang X.D., *Design of Interference Fits via Finite Element Method*, International Journal of Mechanical Sciences, 42, pp. 1835-1850, 2000.

[4] Pimsarn, M., Kazerounian, K., *Efficient evaluation of spur gear tooth mesh load using pseudo-interference stiffness estimation method*, Mechanism and Machine Theory, 37(8), pp. 769-786, 2002.

[5] He, G.P., Hu, C.B., Jin, L.,Yan, C., An, Z.W., Duan, H.Y., *Investigation of mathematical model for machining of externally meshed noncircular gears and characteristics of their undercut,* Journal of Lanzhou University of Technology, 2006;

[6] Berbinschi, S., Teodor, V., Oancea, N., *Kinematical Method for Rack-gear Tool's profiling in CATIA Design Enviroment*, International Journal of Modern Manufacturing Technologies, ISSN 2067–3604, Vol. II, No. 2, pp. 23-30, 2010.

[7] Baroiu, N., Teodor, V., Oancea, N., *A new form of in-plane trajectories theorem. Generation with rotary cutters*, Bulletin of the Polytechnic Institute of Iasi, Tome LXI (LXV), Fascicle 3, section Machine Construction, ISSN 1011-2855, pp. 29-36, 2015.

[8] Markowski, T., Batsch, M., *Tooth Contact Analysis of Novikov Convexo-Concave Gears*, Advances in Manufacturing Science and Technology, vol. 39, no. 1, 2015, doi: 10.2478/amst-2015-0004.

[9] Radzevich, S. P., *Kinematic geometry of surface machining*, CRC Press, Taylor & Francis Group LLC, ISBN 978-1-4200-6340-0

[10] Piska, M., Sliwkova, P., Surface Parameters, Tribological Tests and Cutting Performance of Coated HSS Taps, Procedia Engineering 100 (2015) 125 – 134